CFSRC COLLOQUIUM

Proceedings of the Cold-Formed Steel Research Consortium Colloquium
20-22 October, 2020 (cfsrc.org)

System analysis of nonsymmetric cold-formed steel cross sections members

Edward J. Sippel[1], Hannah B. Blum[2]

Abstract

Cold-formed steel components exist in a variety of structural systems. Wall systems and floor systems are often composed of channel members, and metal building systems often consist of channels or Z-section purlins to construct the wall girts and roofing systems. A common feature of these cross-sections is that they are often open and singly symmetric or point symmetric. While design requirements for these cross-sections account for the relevant effects resulting from their lack of symmetry, structural analysis programs do not always consider these effects. Engineers will use structural analysis programs to calculate the appropriate load sharing among members in the structural system. Accounting for the appropriate stiffness of each member and the related deformations is a vital component to determining the final distribution of bending moment, forces, and displacements. Many common structural analysis programs treat all sections as doubly symmetric without warping. Removing this assumption and considering asymmetry causes non-symmetric cross-sections to exhibit different displacements and complicates the stability limits. The evaluation of these sections is commonly no longer limited to a single plane. The additional displacements directly affect the stability equations, such as the lateral torsional buckling of a beam through the Wagner section parameters, which are all zero for doubly symmetric sections. The analysis of two structural systems composed of nonsymmetric members was completed with varying member modeling assumptions utilizing multiple finite element software programs. A single channel portal frame was investigated that was subjected to simulated gravity load and wind loading with varying bracing support. Additionally, a roofing system with Z-section purlins and channel bracing was investigated. The finite element analyses results were compared among the various modeling assumptions and existing experiments where applicable. It was observed that as deformations and loading increased, the inclusion of non-symmetric section properties becomes more important to ensure an accurate solution is calculated.

1. Introduction

Cold-formed steel sections have thin walls and are often not doubly symmetric which results in complex structural behavior that cannot be fully defined by the base behavior introduced in a Mechanics of Materials course. The AISI Specification [1] identifies some of the complex behavior through the required design capacity provisions. These provisions include requirements accounting for warping and the associated additional normal stresses, the effects of a nonconcentric shear center and centroid for a column buckling under axial load, and Wagner coefficients when defining the lateral torsional buckling capacity of a beam in bending. Other behaviors such as local and distortional buckling effects are also covered.

In contrast, the requirements for the elastic analysis of the structure detailed in Chapter C of the AISI Specification [1] do not cover the same scope of behaviors. Chapter C lists six requirements for the evaluation of cold-formed steel structures with the first two identifying the behavior that must be included. The Specification states the need to consider flexural, shear, and axial member deformations as well as effects of connection deformations with second-order effects highlighting the inclusion of P-δ and P-Δ effects. Within this section of the Specification, there is not an explicit statement regarding the consideration of twist or non-symmetric section properties. The engineer is left to their own discretion for any consideration of twist including warping effects and second-order twist effects with a brief note in Appendix 2 of the Specification related to buckling strength indicating that excluding these effects might not capture the appropriate behavior. Ziemian et. al [2] showed how the twisting of doubly symmetric sections can result in significantly different results. This similarly can occur in non-symmetric sections as they rotate which is amplified by their default behavior. Non-symmetric sections are often not loaded in alignment with a single principal axis nor loaded through the shear center

[1]Graduate Research Assistant, Department of Civil & Environmental Engineering, University of Wisconsin-Madison, esippel@wisc.edu
[2]Assistant Professor, Department of Civil & Environmental Engineering, University of Wisconsin-Madison, hannah.blum@wisc.edu

which introduces an initial out-of-plane deformation.

In addition to the decisions made by the engineer as to what is critical to include, the engineer is often limited to the abilities of the structural analysis software available to them. Many structural analysis programs utilize a beam (line) element that assumes a doubly symmetric cross section with six degrees of freedom per end of the element regardless of the actual shape. Non-doubly symmetric cross sections are allowed to be used within these programs, but limitations exist. The underlying mechanics of the members are typically assumed to still behave the same as a doubly symmetric section based on the principal orientation. The consideration of what effect the nonconcentric shear center and centroid have is left to the user to decide the appropriate alterations to make to a typical model with some direction from design guides, help forums, and experience. The members are often treated as linear for torsion excluding warping effects. The AISI Specification [1] requires the use of warping when evaluating cross sections for the Direct Strength Method and highlights its significance in multiple provisions, but warping is not required as part of the base structural analysis. Recent work by Liu et. al [3], [4] defined a new line element that removes the doubly symmetric assumption and directly accounts for the different behavior of non-symmetric sections. This element has been implemented into MASTAN2 [5] with additional tools to readily model non-symmetric sections.

In this study a comparison of the different results from the structural analysis of non-symmetric sections is presented. The focus of the study is on comparing how the results of a structural system would vary based on the analysis approach utilized. While all analyses completed would meet the requirements of Chapter C, this project considered different analysis methods including first treating all sections as doubly symmetric without warping effects and then other methods that accounted for warping and the non-symmetric section behavior. The systems considered for this project included a single channel portal frame with connection discontinuities and a roof system containing Z-section purlins with discrete channel braces.

2. Structural Analysis Methodology

Many different options and methods are available to engineers to complete their structural analysis. A common approach for practicing engineers is to use a commercially available structural analysis program that implements a line element that assumes a doubly symmetric cross section. This project included results from both SAP2000 [6] and RFEM [7] to represent this possibility. Another approach would be to utilize a method that does not assume doubly symmetric sections. One method available within many structural analysis programs would be to use shell or solid elements to build the model. This was considered for this project using Abaqus [8] to create shell element models for each problem. However, even a small structure modeled this way would become unwieldy quite quickly; therefore a line element model that removes the doubly symmetric assumption would be an alternative to not substantially change from common current modeling procedures. This project chose to employ MASTAN2 [5] and Abaqus as two programs that allow for the inclusion of asymmetric properties while using line elements. When identifying the results in tables and graphs, line element models will be identified by the program name and the shell element model in Abaqus will be identified by the label “shells”.

All of the structural analysis methods considered are capable of capturing flexural, shear, and axial member deformations with consideration of P-δ and P-Δ effects [9]. Typically, the evaluation of these responses is highlighted in two dimensional problems which exclude the impacts of twisting. The effects of twisting exist in three dimensional analyses which are accurately included by all the structural analysis methods considered here. The main difference among the methods is whether or not warping effects are included as part of the torsion analysis. Ignoring the effects of warping is often considered conservative for the analysis of hot-rolled steel sections as discussed in [2]. Ignoring the effects of warping will result in a softer twist response. The analyses previously completely illustrated that cold-formed sections with relatively larger impacts on torsional stiffness from warping could have unexpected behaviors such as reduced or negative lateral deflections when warping effects are ignored [9].

3. Portal Frame

A series of single bay, single channel portal frames was experimentally tested by [10]. Figure 1 shows the left-hand side of the frame geometry which would be mirrored about the center-line to obtain the full frame. The frame was subjected to three loading combinations illustrated in Figure 2 representing vertical only loading (Case 1), transverse wind loading (Case 2), and longitudinal wind loading (Case 3) with one of two lateral support conditions. The first condition provided support at the external lateral bracing locations only, while the second condition provided support at the external and internal lateral bracing locations. The external lateral support was applied at the locations marked by a • in Figure 1 to simulate purlins and girts. The addition of the interior supports at the locations marked with an ‘x’ simulated fly-bracing by introducing a torsional restraint to the channels due the second lateral support. The loading shown in Figure 2 was applied at the same location as the external lateral support. The frame was constructed with lipped channels as the main members and custom bracket connections with the cross-section dimensions shown in Figure 3 [11]. Due to the significantly thicker and larger sections used in the brackets, the apex and eave connections were assumed to be rigid as

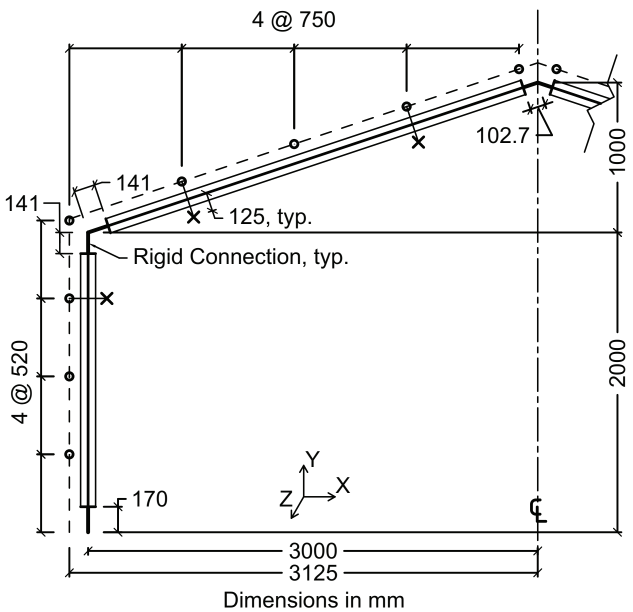

Figure 1: Single channel portal frame geometry. Dimensions shown are symmetric

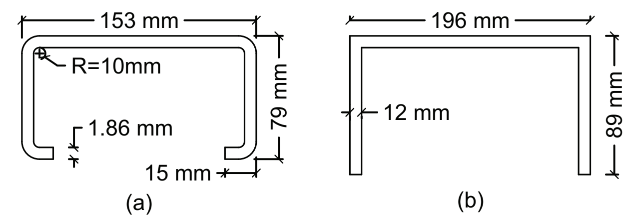

Figure 3: Cross-sectional dimensions of (a) lipped channel and (b) bracket

done in analysis work by [10].

The line element models of the channel portal frames were defined to best reproduce features of the modeling completed by [10] that complemented the physical experiments. The channels were assumed to be connected at the eave and apex by rigid connections that would transfer all moments and forces but allowed for the end of the channels to warp. The channels were modeled to extend to the center of the connection bolts. The previous work utilized the middle of the web of the channel as the origin, therefore this analysis located channel to channel connections at this location as well as the base hinge. The base hinge connection was modeled as only free to rotate about the z-axis. All lateral supports were only capable of a force in the z-direction. The support was modelled at 125 mm perpendicular from the centerline of the channel in the xy-plane and offset in the z-direction to the middle of the flange via a rigid link. The line elements were meshed uniformly between critical dimensions with a reference size of 50 mm based on the mesh study completed as part of a related project [9]. The modulus of elasticity was taken as 203 GPa with a Poisson's ratio of 0.3.

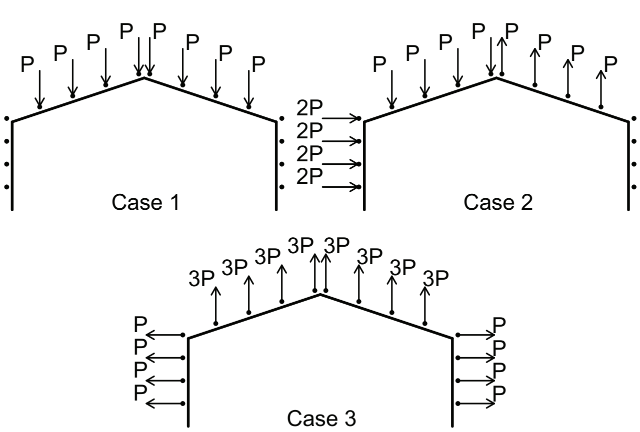

Figure 2: Three loading scenarios applied to portal frame

The shell element models were modeled in an attempt to replicate the modeling assumptions of the line element models. The rigid connection at the ends of the channel with free warping was created by rigid connections to the web of channels. The rigid connection on the web was extended from the end of the member along two line segments up the length of the channel to ensure weak axis moment transfer. The line segments were located at the position of the connection bolts 40 mm to each side of the center-line and extended 60 mm along the length of the member corresponding to the distance between the bolts vertically as illustrated in Figure 4. The base and eave connections were construction with rigid links for the remainder of the joint. The apex connection required the inclusion of a shell model of the connection itself to allow for the multiple boundary conditions on that segment. The lateral supports and loading was applied via a 12 mm thick tab directly tied to the flat of the channel flange. The shell element was meshed with a seed size of 2 mm.

The model was loaded in an undeformed configuration with the experimental preload first and then incrementally based on the full loading program. The provided experimental data included two sets of results for the initial load case with limited differences observed in deformations during the elastic portion of the response despite slightly different unintended imperfections [11]. Due to the location of the applied loading on the channels causing the frame to tend to move out of plane from torsion and since no mention of out of plane imperfections were referenced in previous modeling [10], it was determined that working with an undeformed configuration was appropriate to obtain a baseline comparison. The preload consisted of 175 N at each node to be vertically

Table 1: Analysis results for single channel portal frames at P=500 N

Load Case 1 with Exterior Lateral Supports

Results		SAP2000	RFEM	MASTAN2	Abaqus	Shells	Test
Ux-3	(mm)	-1.83 (41.9%)	-1.82 (42.2%)	-2.01 (36.2%)	-2.04 (35.2%)	-3.15	-2.78
Uy-4	(mm)	-3.45 (58.6%)	-3.44 (58.8%)	-5.53 (33.7%)	-5.63 (32.5%)	-8.34	-7.29
My-1	(N-m)	27.2 (172%)	27.2 (172%)	-33.9 (9.8%)	-34.7 (7.7%)	-37.6	-
Uz-4	(mm)	-1.88 (77.9%)	-1.88 (77.9%)	-5.43 (36.3%)	-5.43 (36.3%)	-8.52	-

Load Case 1 with Exterior and Interior Lateral Supports

Results		SAP2000	RFEM	MASTAN2	Abaqus	Shells	Test
Ux-3	(mm)	-1.78 (45.2%)	-1.80 (44.6%)	-1.79 (44.9%)	-1.82 (44.0%)	-3.25	-2.61
Uy-4	(mm)	-3.45 (46.1%)	-3.40 (46.9%)	-3.50 (45.3%)	-3.58 (44.1%)	-6.40	-4.66
My-1	(N-m)	27.1 (171%)	27.1 (171%)	-39.7 (4.2%)	-40.2 (5.5%)	-38.1	-
Uz-4	(mm)	-0.02 (98.7%)	-0.03 (98.1%)	-0.09 (94.3%)	-0.09 (94.3%)	-1.59	-

Load Case 2 with Exterior Lateral Supports

Results		SAP2000	RFEM	MASTAN2	Abaqus	Shells	Test
Uy-4	(mm)	-3.75 (54.8%)	-3.72 (55.2%)	-4.11 (50.5%)	-4.12 (50.4%)	-8.30	-8.14
Fy-6	(N)	-251 (1.2%)	-251 (1.2%)	-252 (1.6%)	-249 (0.4%)	-248	-

Position Number: 1 = Left Base Connection, 3 = Left Eave, 4 = Midspan of Left Rafter, & 6 = Right Base Connection

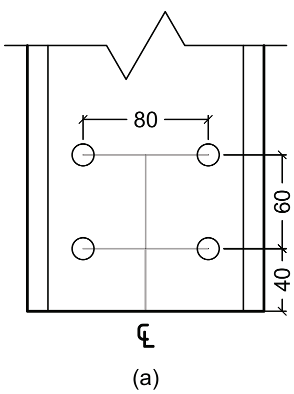

Figure 4: Dimensions of channel (a) end bolted connection and (b) rigid tie model

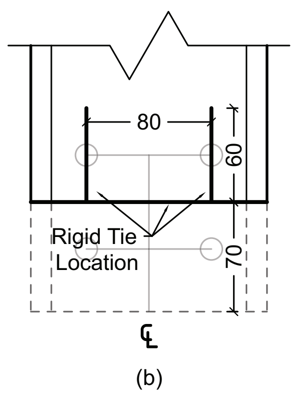

Figure 5: Vertical displacement at midspan of left rafter for Load Case 1

loaded and 10 N at each node to be horizontally loaded in the direction of future loading. After this initial step, the loading was increased at each node corresponding to the loading distribution indicated in Figure 2.

The available experimental data [11] provided the in-plane deformation for most of the test configurations. As shown in Figure 5, it was observed that the shell analysis model was capable of reasonably modeling the main behavior of the frames while most line element models were stiffer. It can been seen that there was a significant difference between the deflection captured by the non-symmetric line element versus the doubly symmetric line element. This variation in the main lateral and vertical response was more pronounced when only external lateral support was applied to the frames versus when the internal lateral support was added to the frames. Table 1 summarizes some of these responses with absolute error to the shell model results provided in parentheses after the numeric value. Also included in the table are results for the out-of-plane deflection from the model evaluations. From this data, it is of particular interest that the doubly symmetric analysis programs are typically calculating less deflection out-of-plane than the non-symmetric analysis particularly when the frame was only laterally supported by the external braces.

The results from this study were found to stiffer than those from the results plotted by [12]. In an attempt to understand the difference between the results of this study with non-symmetric analyses and the prior study's values, the structural analysis procedures were reviewed. The primary difference noted between these methods was the transfer of forces at the connections. The methods used in this study have no specific mechanism for the transfer of bimoment around a section at the connections other than continuous, fixed, or free for warping. The work by [12] similarly had the ends of members defined as continuous, fixed, or free for warping, but additionally included a factor for bimoment to be developed due to the internal bending moments and differences between the shear center locations between elements. While not fully explored in this study, it was observed that pattern of bimoment identified by [12] could not be reproduced within MASTAN2 or Abaqus line elements as currently utilized as there is no connection between the bimoment and the bending moments within the rigid link connection nor the initial transformation of forces to the line elements.

4. Roof System

A single slope roof as shown in Figure 6 was evaluated for the interactive effect between the non-symmetric roof members and doubly symmetric supporting I-beams. The cross-section designations that follow are listed by the equivalent metric size followed by the standard American section size. The sloped roof consists of four W310x38.7 (W12x26) I-beams supporting continuous Z-section purlins, 305Z76-254M (1200Z300-100). Unlike many roof systems that use continuous bracing, the purlins were assumed to be discretely braced at the midpoint by a series of channels, 203S70-144M (800S275-57), following the research completed by [13] that a single brace could adequately constrain the twist of the purlins. The I-beams were supported in the vertical direction at each end and supported in the lateral directions as shown in Figure 6. Indicated by the •'s in Figure 6(a), fly bracing from the center of the web of the purlin to the bottom flange of the I-beam was created with L51x51x3.2 (L2x2x1/8) angles to provide torsional stability. The I-beam and angle members were modeled with a modulus of elasticity of 200 GPa and the Z-section and channel members were modeled with a modulus of elasticity of 203 GPa. All members were modeled with a Poisson's ratio of 0.3.

The roof purlins were modeled as continuous in a prismatic condition. In roof purlin design, it is often considered conservative and more accurate to use a nonprismatic condition for the lapped dimension due to the fact that the capacity of the purlin is controlled by the negative moment region at the support and the increased stiffness of a nonprismatic condition at the support would cause a larger negative moment [14]. As a consequence, the maximum positive moment decreases which is not controlling the design due to the typical assumption that the purlin is continually braced and will reach the yield moment capacity. However, in this analysis it was desired to calculate the largest possible positive moment along the span as the purlins are considered to be unbraced and the member is controlled by lateral torsional buckling. The purlins were assumed to be simply supported

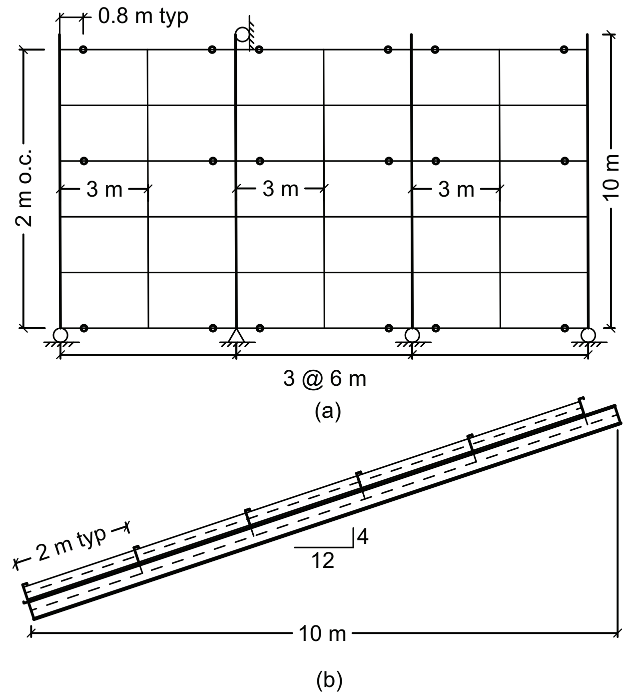

Figure 6: Roof layout (a) Plan view (b) Section view

for strong and weak axis moment at all connections to the beam while still transferring torsion from the Z-section purlin to the I-beam and was free to warp at the ends. The channel braces were assumed to only be connected via the web which corresponded with releasing the weak axis moment at the connection and the end of the channel being free to warp. The Z-section purlin and channel braces were modeled with sharp corners. In the various models, rigid links were used to allow for the purlins to be stacked above the beams and still transfer loading. The line element models were meshed with a seed of 200 mm, and the shell element model was meshed with a seed of 5 mm.

The roof system was evaluated for the application of a downward vertical load simulating dead/live loading and an upward load perpendicular to the roof slope to simulate wind loading. A uniform distributed load was assumed to be applied to the centroid of all purlins. The line element models allowed for the direct application of a distributed load. The shell element model was loaded with discrete point loads at all nodes along the centerline of the purlin based on the length of the element. The evaluation of the roof system first considered the performance of the roof system at a 1.5 kN/m distributed loaded. An additional comparison was completed that determined the maximum distributed load that could be applied to the roof system prior to any instabilities were identified.

For the current work, the comparison of the demand capac-

Table 2: Analysis results for roof system with 1.5 kN/m distributed load

Downward Loading

Results	SAP2000	RFEM	MASTAN2	Abaqus	Shells
Beam Mx (N-m)	59551 (2.1%)	59600 (2.0%)	59526 (2.1%)	59197 (2.7%)	60810
Beam Uy (mm)	38.3 (2.0%)	38.0 (2.8%)	37.9 (3.1%)	38.0 (2.8%)	39.1
Purlin Uy (mm)	41.0 (5.7%)	40.6 (6.7%)	40.7 (6.4%)	40.9 (6.0%)	43.5
Purlin 1 Ratio	37.6%	35.9%	32.8%	33.0%	37.5%
Purlin 4 Ratio	33.0%	28.7%	22.6%	23.1%	21.4%

Uplift Loading

Results	SAP2000	RFEM	MASTAN2	Abaqus	Shells
Beam Mx (N-m)	63297 (1.7%)	63331 (1.7%)	63193 (1.9%)	62935 (2.3%)	64420
Beam Uy (mm)	40.9 (1.9%)	40.5 (2.9%)	40.3 (3.4%)	40.4 (3.1%)	41.7
Purlin Uy (mm)	43.2 (2.9%)	42.8 (3.8%)	42.9 (3.6%)	43.1 (3.1%)	44.5
Purlin 1 Ratio	36.2%	36.6%	35.1%	35.9%	34.2%
Purlin 4 Ratio	45.5%	44.5%	43.1%	43.4%	44.4%

ity ratio in purlins was focused on the interaction of strong and weak axis moment. The AISI Specification [1] would also require the evaluation of the combined effects of moment and each of the following effects separately: shear, web crippling, and torsion. Based on initial evaluations utilizing a simple continuous beam, it was found that at the load level considered shear and web crippling would not control. The effects of warping and torsion would cause additional normal stresses that would add to the bending moment effects, but the rational analysis method suggested in the AISI commentary allows for this interaction to be completed based on the local buckling capacity of the section and not to be combined with the reductions for global effects which resulted in a less critical condition. The moment demand capacity ratio comparisons utilized the Direct Strength Method moment capacity of the purlins calculated using sharp corners in CUFSM [15]. The capacities were calculated for an unbraced length of 3 m based on the principal orientation of the Z-section [16].

The results of the load cases with a finite 1.5 kN/m loading found similar results among all the analysis methods considered when comparing the maximum vertical deflections, the moment along the supporting I-beams, and the demand capacity ratio for the purlins considering major and minor axis bending with a sampling shown in Table 2. The values in parentheses are the absolute error relative to the shell result. The provided purlin ratio checks were completed for the controlling midspan moments. It was found that the positive midspan moment was the controlling location for moment magnitudes in the purlins. The first purlin, which is the purlin at the lowest elevation, experienced larger negative moments at the support due to the absence of differential displacements at the support beams; however, the consideration of this load being shared between the two lapped purlins at this location resulted in a reduced demand capacity ratio at the support compared to midspan. It was also observed that the negative moment in the purlins decreased as the differential deflection of the support beams increased further causing the positive moment to control.

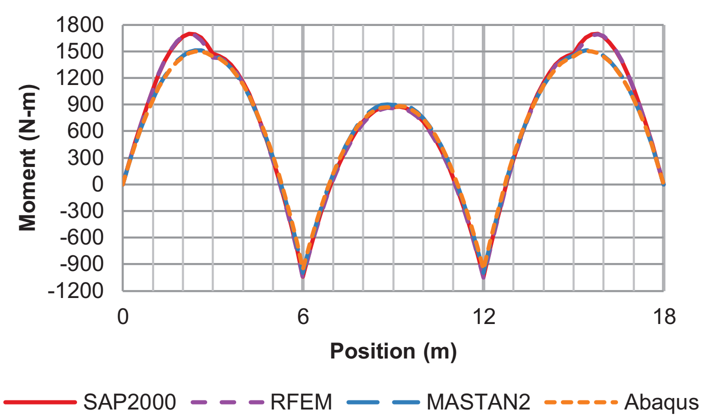

Figure 7: Geometric weak axis moment from vertical loading along 4th purlin. Position = 0 is the left side of Figure 6a

Despite the agreement among the methods shown thus far, the results were not identical. Using the fourth purlin as a reference, the major axis moment in both scenarios matched well between the different line element analysis methods. The weak axis moment experienced more variation as shown in Figure 7 and Figure 8. Due to the combination of the roof slope and the member geometry, the downward vertical load was oriented 7° closer to the principal orientation resulting in less rotation compared to the uplift load. The softer torsional response from excluding warping effects in the doubly symmetric analysis resulted in a higher variability as the section exhibited larger twists.

The evaluation of the roof systems to find a maximum loading exhibited significant differences among the analysis methods. The maximum loading was found via a nonlinear static analysis with the results summarized in Table 3 as well as eigenbuckling with MASTAN2 and Abaqus. An eigenbuckling analysis of the shell element model found that the roof system was capable of supporting 3.7 kN/m downwards at which point the full roof system should buckle laterally and

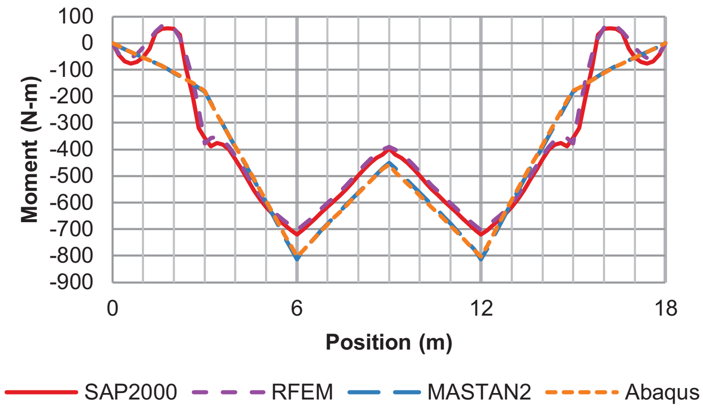

Figure 8: Geometric weak axis moment from uplift loading along 4th purlin. Position = 0 is the left side of Figure 6a

Table 3: Maximum distributed load applied [kN/m]

Case	SAP2000	RFEM	MASTAN2	Abaqus	Shells
Down	1.67	1.80	3.63	3.58	3.78
Uplift	1.80	1.92	3.99	4.03	3.42

3.3 kN/m in uplift when the interior beams should experience lateral torsional buckling. The non-symmetric line element analysis found similar failure modes, but at slightly different values of 3.5 kN/m downwards and 3.8 kN/m in uplift. An evaluation of the the roof system as doubly symmetric elements without warping effects found that the bracing channels were controlling the analysis at reduced maximum loads of 1.3 kN/m downwards and 1.6 kN/m in uplift. The nonlinear analysis utilizing the various programs captured similar behavior. It was determined that the nonlinear analysis was indicating an instability if the model was exhibiting significant change in deformations or if the model would fail to converge with either a reference to a negative or zero stiffness value or indicating deformations corresponding to the eigenbuckling analysis failure mode of similar loading magnitude. The shell and non-symmetric line element analyses found the appropriate buckling failure with only a slight increase in the maximum load applied. The greatest variation was observed with the doubly symmetric line element analyses. The methods used were capable of analyzing past the point of the first channel buckling without significant variation in deformations; however, the system quickly became unstable for additional loading. The loss of an effective intermediate brace plus the exclusion of the warping stiffness resulted in premature failure of the purlins.

5. Discussion

The evaluation of structural systems requires accounting for the appropriate load sharing and deformation of the various elements of that structure. The use of non-symmetric cross sections within a structure present a challenge due to the increased complexity of their deformation behavior. Many applications including these cross sections will introduce twisting to the structural analysis problem which can cause significant differences. As shown in the single channel portal frame examples, the more freedom a member has to rotate the more critical it is to capture the true behavior of non-symmetric sections to obtain the appropriate response. In applications where additional restraint exists, a doubly symmetric analysis does a better job approximating the non-symmetric behavior. However at large loading values, the exclusion of the non-symmetric behavior becomes more significant as the doubly symmetric analysis does not capture the same twist-shear-bending interactions of the member.

The overall result when not accounting for the non-symmetric behavior of cross sections was observed to be both conservative and unconservative. As was shown in the single channel portal frame, an assumption of doubly symmetric behavior resulted in a stiffer response for the overall deflection of the frame compared to when the non-symmetric behavior was included. Even though the doubly symmetric analysis did not account for the effects of warping which should have caused additional rotation, the exclusion of non-symmetric behavior including the torsional considerations from the shear center being nonconcentric with the centroid caused the channel members to rotate less out-of-plane. After applying the additional internal support, the variation in the overall response of the frame was decreased. When working with the roof system example, the results among the different analysis methods had minimal differences at lower loading levels. However, most structures are not designed to be utilizing a member at less than 50% of the available strength. The double symmetric analysis indicated a relatively conservative result that the maximum load could have only been increased by 11% - 28% before stability issues arose, whereas realistically the system could support more than double the initial condition.

This result that the differences between non-symmetric analyses and doubly symmetric analyses can be conservative or unconservative means that the ability of an engineer to determine what is critical to include when considering the analysis of non-symmetric sections is increasingly important and difficult. Depending on the exact goals and type of structure to be evaluated, the minimum requirements of a structural analysis given in AISI Specifications Chapter C provide an useful baseline, but the analysis of non-symmetric cross sections is significantly affected by twisting and second-order twisting effects that are not currently listed in the specification. When including the AISI Specifications and twisting effects in a doubly symmetric analysis, it may be capable of determining similar results to a more complete non-symmetric analysis when calculating deformation and internal forces. However, this should be a conscious decision made by the engineer, not a consequence of following the minimum requirements.

6. Conclusion

Two structural systems with non-symmetric sections were evaluated with various finite element models to observe the importance of the inclusion of non-symmetric section properties in the analysis of those systems. Depending on the exact goals and type of structure to be evaluated, the minimum requirements of a structural analysis given in the AISI Specification Chapter C provide a useful baseline, but the analysis of non-symmetric cross sections is significantly affected by twisting and second-order twisting effects that are not currently listed in the specification. It was observed that when the allowable rotation of a member was limited the results of a structural analysis assuming doubly symmetric sections were more closely aligned with an analysis that considered non-symmetric section effects. The variations between these different analysis methods were found to be both conservative and unconservative and the cumulative effect of the different underlying mechanical behavior within the system could not be readily predicted.

7. Acknowledgments

The authors would like to thank Professor Ronald Ziemian at Bucknell University and Professor Siwei Liu and his research team at Sun Yat-Sen University for their assistance with the updated MASTAN2 program.

References

[1] AISI S100-16, *North American Specification for the Design of Cold-Formed Steel Structural Members*. Washington, DC, U.S.A.: AISI, 2016.

[2] R. D. Ziemian, J. C. Batista Abreu, M. D. Denavit, and T.-J. L. Denavit, "Three-Dimensional Benchmark Problems for Design by Advanced Analysis: Impact of Twist," *J. Struct. Eng.*, vol. 144, no. 12, p. 04 018 220, 2018, ISSN: 0733-9445. DOI: 10.1061/(asce)st.1943-541x.0002224.

[3] S.-W. Liu, W. L. Gao, and R. D. Ziemian, "Improved line-element formulations for the stability analysis of arbitrarily-shaped open-section beam-columns," *Thin-Walled Struct.*, vol. 144, no. July, p. 106 290, 2019, ISSN: 02638231. DOI: 10.1016/j.tws.2019.106290. [Online]. Available: https://doi.org/10.1016/j.tws.2019.106290.

[4] S.-W. Liu, R. D. Ziemian, L. Chen, and S.-L. Chan, "Bifurcation and large-deflection analyses of thin-walled beam-columns with non-symmetric open-sections," *Thin-Walled Struct.*, vol. 132, no. 135, pp. 287–301, 2018, ISSN: 02638231. DOI: 10.1016/j.tws.2018.07.044. [Online]. Available: https://doi.org/10.1016/j.tws.2018.07.044.

[5] R. D. Ziemian, W. McGuire, and S.-W. Liu, *MASTAN2*, 2019.

[6] CSI America, *SAP2000*, Berkeley, CA, 2018.

[7] Dlubal Software, *RFEM 5 User Manual*, December 2. Dlubal Software GmbH, 2019, p. 650.

[8] Dassault Systems, *Abaqus/CAE*, Johnston, RI, 2015.

[9] E. J. Sippel, R. D. Ziemian, and H. B. Blum, "Analysis of non-symmetric cross-sections relative to the provisions of AISC 360-10," in *Struct. Stab. Res. Counc. 2020 Annu. Stab. Conf.*, SSRC, Ed., Atlanta, GA, 2020, pp. 1–28.

[10] A. H. Baigent and G. J. Hancock, "Structural analysis of assemblages of thin-walled members," *Eng. Struct.*, vol. 4, no. 3, pp. 207–216, 1982, ISSN: 01410296. DOI: 10.1016/0141-0296(82)90010-4.

[11] A. H. Baigent, "Thin-Walled Structural Systems," PhD thesis, The University of Sydney, 1980, pp. 291–610.

[12] A. H. Baigent and G. J. Hancock, "The Stiffness and Strength of Portal Frames Composed of Cold-Formed Members," *Civ. Eng. Trans.*, vol. 24, no. 3, pp. 278–283, 1982.

[13] T. Sputo, J. Haynes, and D. S. Ellifritt, "Flexural Capacity of Discretely Braced C' s and Z' s," *11th Int. Spec. Conf. Cold-Formed Steel Struct.*, vol. 2, pp. 109–129, 1992. [Online]. Available: https://scholarsmine.mst.edu/isccss/11iccfss/11iccfss-session3/2.

[14] H. I. Epstein, E. Murtha-Smith, and J. D. Mitchell, "Analysis and design assumptions for continuous cold-formed purlins," *Pract. Period. Struct. Des. Constr.*, vol. 3, no. 2, pp. 60–67, 1998, ISSN: 10840680. DOI: 10.1061/(ASCE)1084-0680(1998)3:2(60).

[15] Z. Li and B. W. Schafer, "Buckling analysis of cold-formed steel members with general boundary conditions using CUFSM: Conventional and constrained finite strip methods," in *20th Int. Spec. Conf. Cold-Formed Steel Struct. - Recent Res. Dev. Cold-Formed Steel Des. Constr.*, 2010.

[16] S. Wang, R. S. Glauz, and B. W. Schafer, "Inelastic Lateral-Torsional Buckling Strength Validation for Non-Principal Axis Bending Using Numerical Methods," Tech. Rep., 2020, p. 62.